A 3-DIMENSIONAL FINITE-DIFFERENCE METHOD FOR CALCULATING

THE DYNAMIC COEFFICIENTS OF SEALS

F.J. Dietzen and R. Nordmann
Department of Mechanical Engineering
University of Kaiserslautern
Kaiserslautern, Federal Republic of Germany

This paper presents a method to calculate the dynamic coefficients of seals with arbitrary geometry. To describe the turbulent flow the Navier-Stokes equations are used in conjunction with the k-ε turbulence model. These equations are solved by a full 3-dimensional finite-difference procedure instead of the normally used perturbation analysis. The time dependence of the equations is introduced by working with a coordinate system rotating with the precession frequency of the shaft. The results of this theory are compared with coefficients calculated by a perturbation analysis and with experimental results.

INTRODUCTION

During the last years it has become evident that it is important to include the fluid forces caused by seals when predicting the dynamic behavior of turbopumps. To calculate these forces and the dynamic coefficients which are normally used to describe them (eq. 1)

$$- \begin{bmatrix} F_z \\ F_y \end{bmatrix} = \begin{bmatrix} K & +k \\ -k & K \end{bmatrix} \begin{bmatrix} z \\ y \end{bmatrix} + \begin{bmatrix} D & d \\ -d & D \end{bmatrix} \begin{bmatrix} \dot{z} \\ \dot{y} \end{bmatrix} + \begin{bmatrix} M & m \\ -m & M \end{bmatrix} \begin{bmatrix} \ddot{z} \\ \ddot{y} \end{bmatrix}$$

several methods which are based either on the so-called "bulk-flow" theories /1,2/ or directly on the Navier-Stokes equations /3,4/ have been published. A common feature of these methods, developed for straight pump seals /1/ straight gas seals /2,4/ or grooved seals /3/, is that they are all based on a perturbation analysis to determine the dynamic coefficients. But the perturbation analysis requires many assumptions, e.g.

1. It is assumed that the shaft moves on small orbits around the centric position, so that a perturbation analysis can be used for all flow variables

$$\phi = \phi_o + e\phi_1 + e^2\phi_2\ldots.$$

and all terms with power of e greater than one can be neglected in the equations without loss of accuracy (e = perturbation parameter).

2. The change of the perturbation flow variables in the circumferential direction can be described by sine and cosine functions.

$$\phi_1 = \phi_{1c} \cos\theta + \phi_{1s} \sin\theta$$

3. The change in time can be described by

$$\phi_1 = \phi_1 \, e^{i\Omega t}$$

because the shaft moves on a circular orbit.

To check how these assumptions effect the results we have developed a 3-dimensional finite-difference procedure to calculate the dynamic coefficients. The only assumptions in this theory are that the turbulence can be described by the k-ϵ turbulence model and that the shaft moves on circular orbits around the seal center.

GOVERNING EQUATIONS

To describe the turbulent flow in a seal we have the Navier-Stokes equations and the continuity equation. The turbulent stresses occurring in the fluid can be handled like laminar stresses by introducing a turbulent viscosity. The turbulent and the laminar viscosity are then summed up to an effective viscosity μ_e

$$\mu_e = \mu_l + \mu_t$$

To describe μ_t the k-ϵ turbulence model /5,6/ is used because it is simple and often used to calculate the turbulent flow in seals /7,8,9,10/.

$$\mu_t = C_\mu \, \rho \, \frac{k^2}{\epsilon}$$

All these equations can be represented in the following form

$$\rho\frac{\partial\phi}{\partial t} + \frac{\partial}{\partial x}(\rho u\phi) - \frac{\partial}{\partial x}(\Gamma_\phi \frac{\partial\phi}{\partial x}) + \frac{1\partial}{r\partial r}(r\rho v\phi) - \frac{1\partial}{r\partial r}(r\Gamma_\phi \frac{\partial\phi}{\partial r}) + \frac{1\partial}{r\partial\theta}(\rho w\phi) - \frac{1\partial}{r\partial\theta}(\Gamma_\phi \frac{1\partial\phi}{r\partial\theta}) = S_\phi$$

ϕ	Γ_ϕ	S_ϕ
u	μ_e	$-\frac{\partial p}{\partial x} + \frac{\partial}{\partial x}(\mu_e\frac{\partial u}{\partial x}) + \frac{1}{r}\frac{\partial}{\partial r}(r\mu_e\frac{\partial v}{\partial x}) + \frac{1}{r}\frac{\partial}{\partial \theta}(\mu_e\frac{\partial w}{\partial x})$
v	μ_e	$-\frac{\partial p}{\partial r} + \frac{\partial}{\partial x}(\mu_e\frac{\partial u}{\partial r}) + \frac{1}{r}\frac{\partial}{\partial r}(r\mu_e\frac{\partial v}{\partial r})$ $+ \frac{1}{r}\frac{\partial}{\partial \theta}(r\mu_e\frac{\partial}{\partial r}(\frac{w}{r})) - \frac{2}{r^2}\mu_e\frac{\partial w}{\partial \theta} - \frac{2}{r^2}\mu_e v + \frac{\rho}{r}w^2$
w	μ_e	$-\frac{1}{r}\frac{\partial p}{\partial \theta} + \frac{\partial}{\partial x}(\frac{1}{r}\mu_e\frac{\partial u}{\partial \theta}) + \frac{1}{r}\frac{\partial}{\partial r}(\mu_e\frac{\partial v}{\partial \theta}) + \frac{1}{r}\frac{\partial}{\partial \theta}(\frac{1}{r}\mu_e\frac{\partial w}{\partial \theta})$ $+ \frac{1}{r^2}\mu_e\frac{\partial v}{\partial \theta} - \frac{w}{r^2}\frac{\partial}{\partial r}(r\mu_e) + \frac{1}{r}\frac{\partial}{\partial \theta}(\frac{2}{r}\mu_e v) - \frac{\rho}{r}vw$
1	0	0
k	μ_e/σ_k	$G - \rho\epsilon$
ϵ	μ_e/σ_ϵ	$C_1\frac{\epsilon}{k}G - C_2\rho\frac{\epsilon^2}{k}$

Table 1: Source terms of the Navier–Stokes equations, the continuity equation and the equations of the k-ε model.
(constants of k-ε model are given in Appendix A)

To determine the dynamic coefficients we assume that the shaft moves on a circular orbit with precession frequency Ω around the seal center. Since this would normally result in a time dependent problem we introduce a rotating coordinate system which is fixed at the shaft center (Fig. 1). In this system the flow is stationary.
Due to the rotating coordinate system centrifugal- and coriolis-forces occur in the equations for the radial and circumferential momentum /11/, which are taken into consideration by a modification of the source terms.

$$S_v' = S_v + \Omega^2 r + 2\Omega w$$

$$S_w' = S_w - 2\Omega v$$

So the final form of the equations is given if S_v and S_w in Table 1 are replaced by S_v' and S_w'.
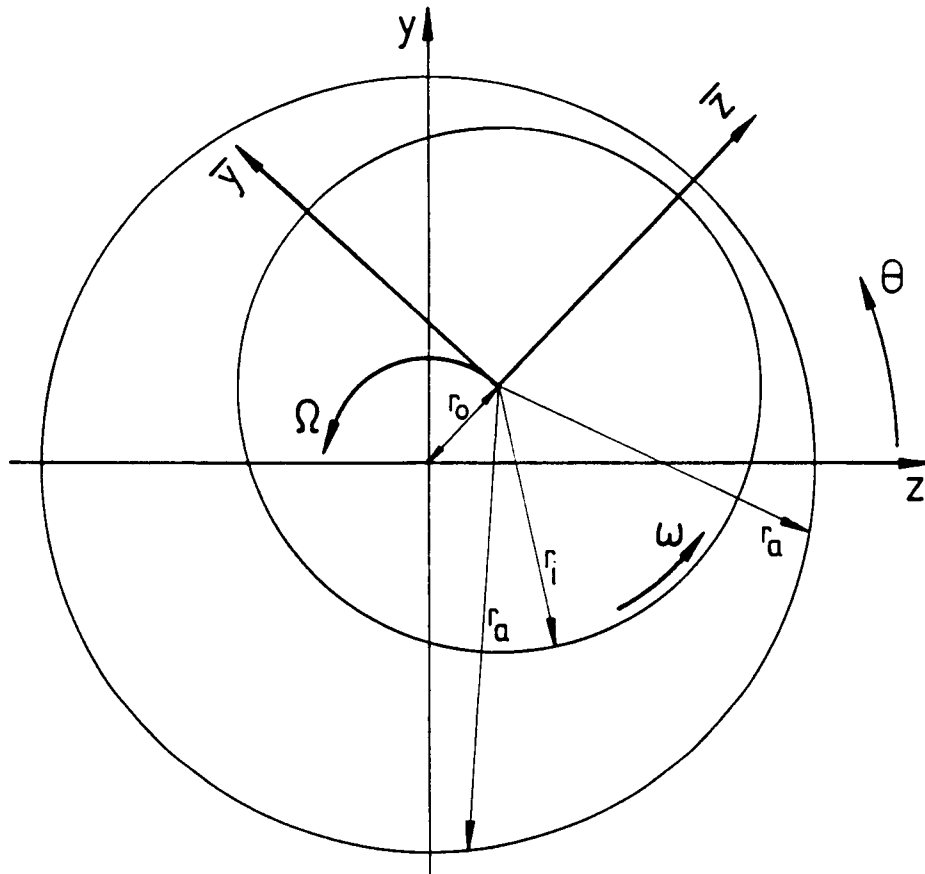
Fig. 1: Rotating coordinate system

BOUNDARY CONDITIONS

The above given equations are solved in conjunction with the following boundary conditions (Fig. 2)
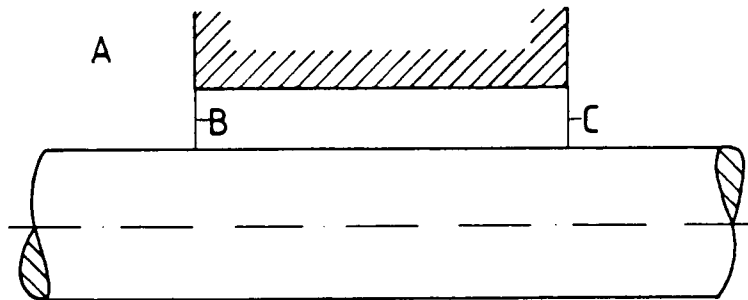

Fig. 2: Locations where the boundary-conditions must be specified

Entrance: $P_{B(\theta)} + \frac{1}{2}\rho\bar{u}^2_{B(\theta)}(1+\xi) = P_A$

Exit : $P_{C(\theta)} = 0$

Stator : $u = 0$ $v = 0$ $w = -\Omega r$

Rotor : $u = 0$ $v = 0$ $w = (\omega-\Omega)r$

$\bar{u}_B$ is the average axial entrance velocity specified for every grid-plane.

For k and ϵ the standard conditions of the k-ϵ model /5,6/ are used at the walls.

FINITE-DIFFERENCE-PROCEDURE

This system of equations with the corresponding boundary conditions is solved by a 3-dimensional finite-difference procedure, based on the method published by Gosman and Pun /12/. The seal is discretized by a grid (Fig. 3) and the variables are calculated at the nodes. To determine the pressure we use the PISO /13/ algorithm instead of SIMPLE /14/.
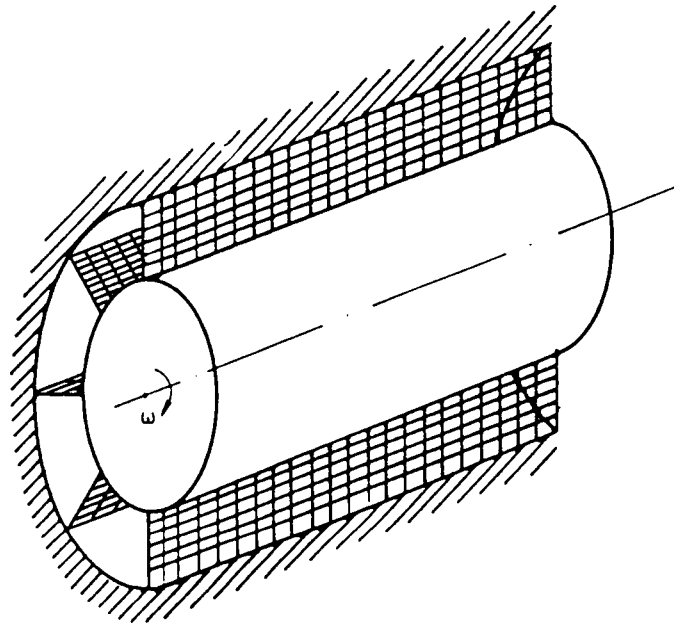

Fig. 3: Mesh arrangement in the seal

DYNAMIC COEFFICIENTS

As result of our solution procedure we get the pressure distribution in the seal and by a pressure integration in axial and circumferential direction, the forces. To simplify the integration we consider the case when the rotating coordinate system $\bar{y}$, $\bar{z}$ coincides with the stationary system y, z.

$$F_z = -\int_o^L \int_o^{2\pi} p\cos\theta \, r_i d\theta dx \qquad\qquad F_y = -\int_o^L \int_o^{2\pi} p\sin\theta r_i d\theta dx$$

When calculating the forces for 3 precession frequencies $\Omega = 0\omega$, $\Omega = 1\omega$ and $\Omega = 2\omega$ we can determine the dynamic coefficients. To save computation time we calculate k, ϵ and μ_t only for $\Omega = 0$ and keep it constant then for $\Omega = 1\omega$ and $\Omega = 2\omega$.

RESULTS

1. Example

First we compare the results of the 3-dimensional theory with those of a method, based on a perturbation analysis in the Navier-Stokes equations and in addition with experimental values.
For a straight seal with the following data the results are shown in Fig. 5.

L = 23.5 mm $\mu_1 = 0.7*10^{-3}$ Ns/m^3

r_i = 23.5 mm ρ = 996.0   kg/m^3

C_o = 0.2 mm $\bar{u}$ = 16.46   m/s

$\bar{w}(0,\theta,2000 \text{ RPM})/r_i\omega = 0.13$ $\xi(2000 \text{ RPM}) = 0.35$

$\bar{w}(0,\theta,4000 \text{ RPM})/r_i\omega = 0.17$ $\xi(4000 \text{ RPM}) = 0.37$

$\bar{w}(0,\theta,6000 \text{ RPM})/r_i\omega = 0.19$ $\xi(6000 \text{ RPM}) = 0.38$

2. Example

For a grooved seal (Fig. 4) the dynamic coefficients are shown as a function of the groove depth H_R (Fig. 6,7).
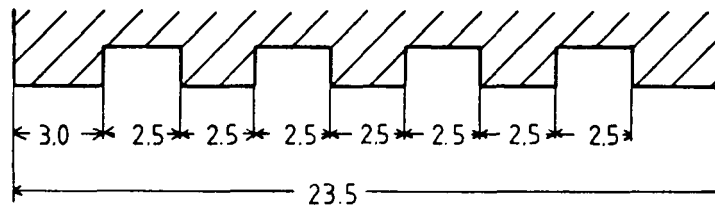

Fig. 4: Geometry of grooved seals

The seal data are

$$L = 23.5 \text{ mm}$$

$$\mu_1 = 0.7 \! * \! 10^{-3} \text{ Ns/m}^3$$

$$r_i = 23.5 \text{ mm}$$

$$\rho = 996.0 \text{ kg/m}^3$$

$$C_o = 0.2 \text{ mm}$$

$$w(0,\theta,\bar{u} = 14.11 \text{ m/s})/r_i \omega = 0.20$$

$$\xi(14.11 \text{ m/s}) = 0.38$$

$$w(0,\theta,\bar{u} = 11.76 \text{ m/s})/r_i \omega = 0.22$$

$$\xi(11.76 \text{ m/s}) = 0.39$$

In Fig. (8.9) the grid, the axial and radial velocity, the circumferential velocity and the pressure are shown for a groove depth of 0.5 mm and an average axial velocity of $\bar{u} = 14.11$ m/s.

3. Example

In some further calculations we have investigated the influence of grooves on the rotor and stator for the seal shown in Fig. 10.

The seal data are

$$L = 35.0 \text{ mm}$$

$$\mu_1 = 0.7 \! * \! 10^{-3} \text{ Ns/m}^3$$

$$r_i = 23.7 \text{ mm}$$

$$\rho = 996.0 \text{ kg/m}^3$$

$$C_o = 0.2 \text{ mm}$$

$$n = 4000 \text{ RPM}$$

$$\xi = 0.5$$

$$\bar{w}(0,\theta) = 0.5 \! * \! r_i \omega$$

groove depth on rotor and stator : 0.4 mm
total pressure loss : 0.8 Mpa
radius of shaft orbit : $r_o = C_o/40$

In Fig. 10 the total stiffness coefficients of the seal, and the portions developed in each part of the seal are shown.
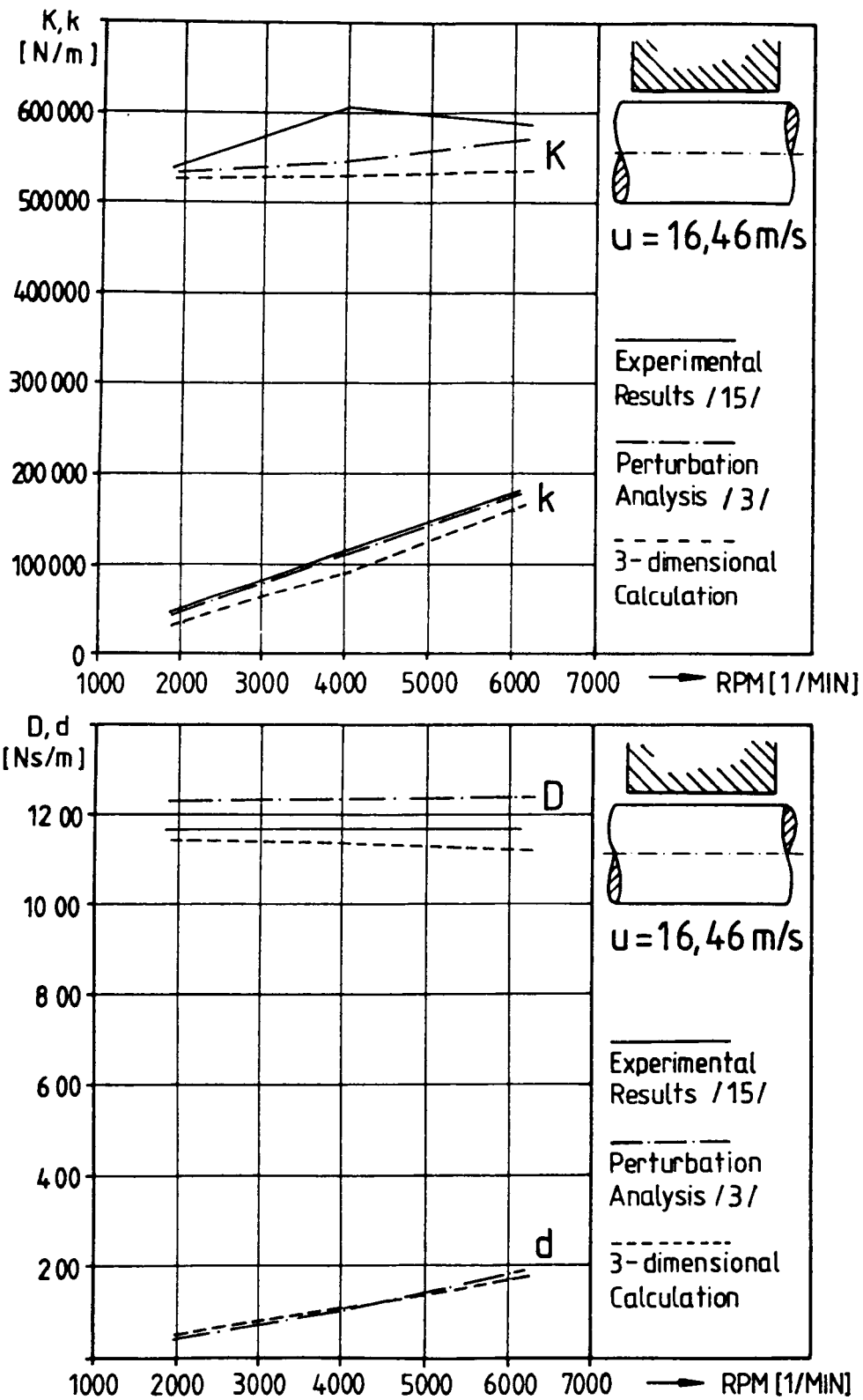
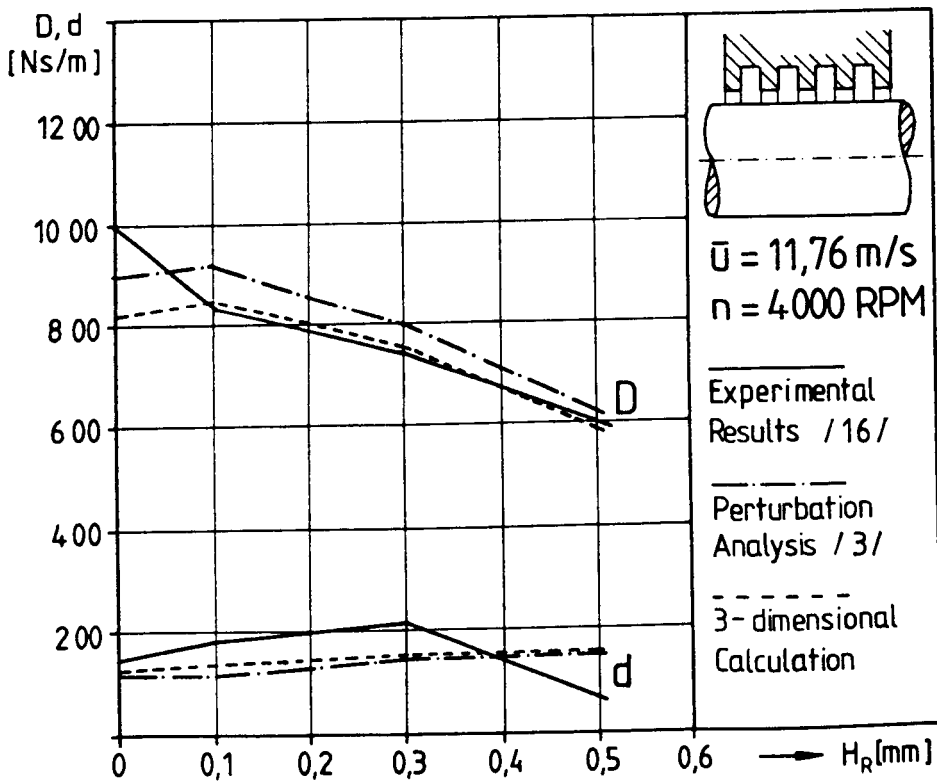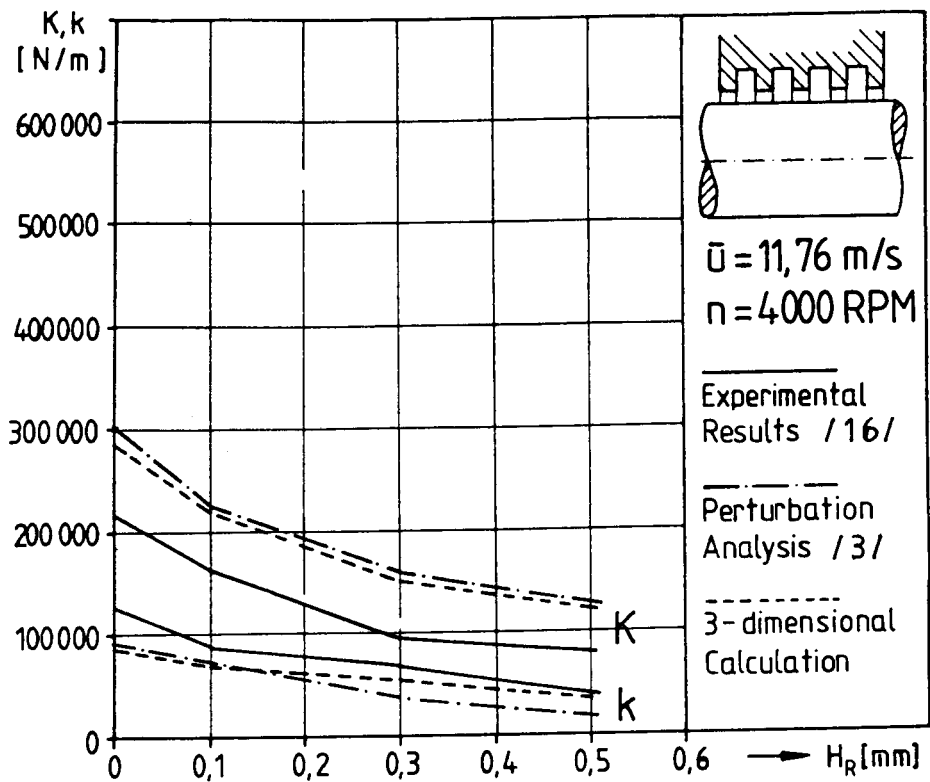Fig. 5: Comparison of the dynamic coefficients for a straight seal.
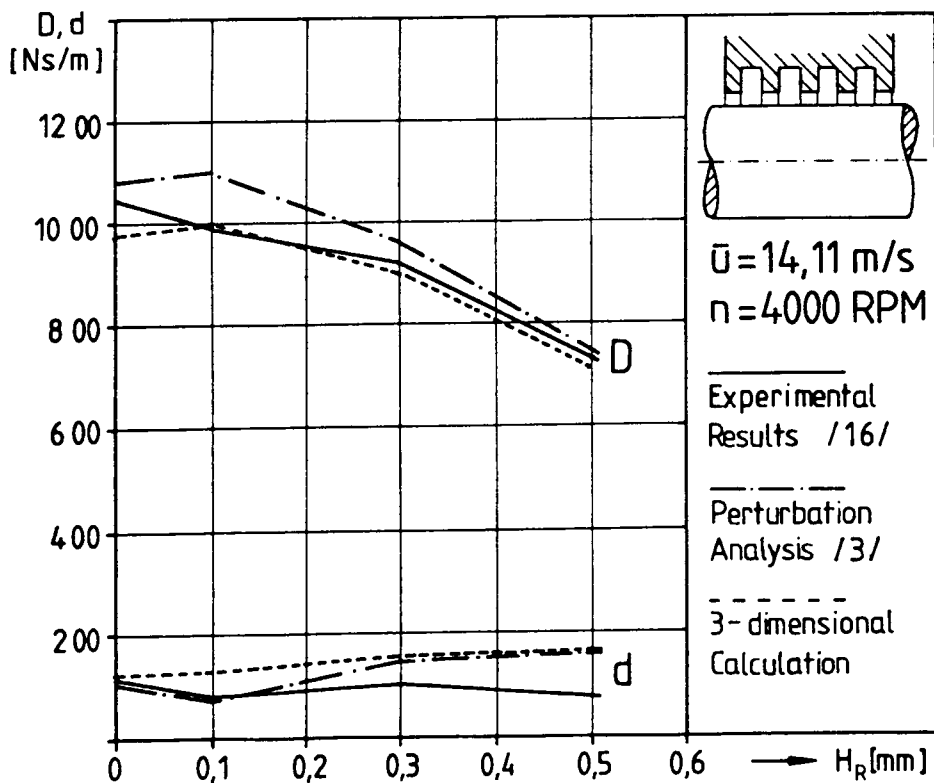
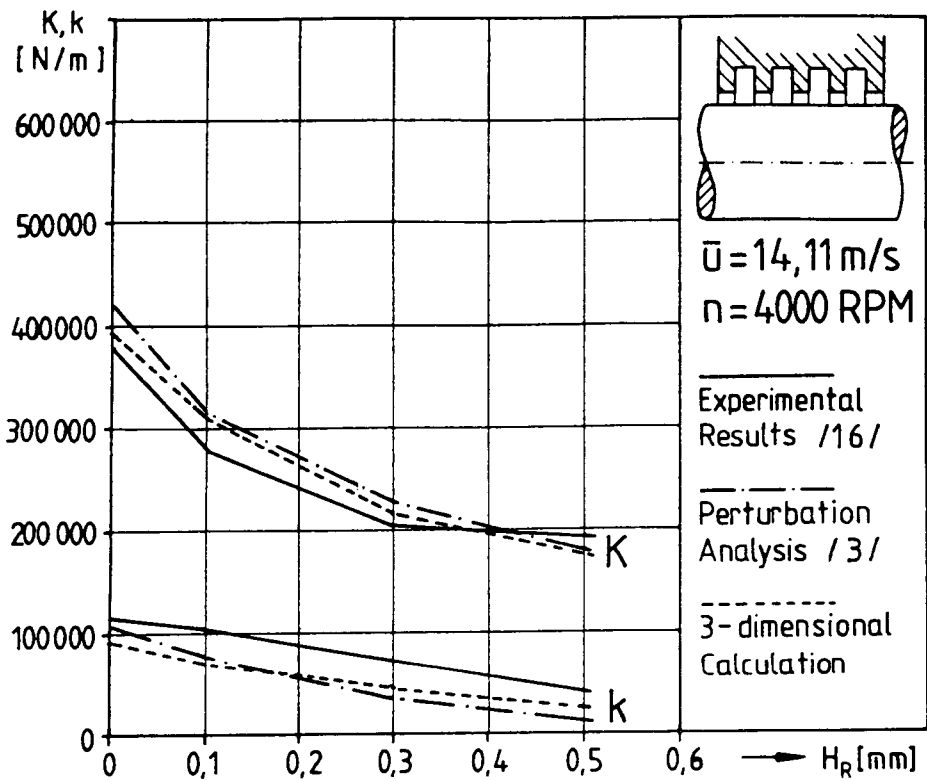Fig. 6: Comparison of the dynamic coefficients for grooved
seals.

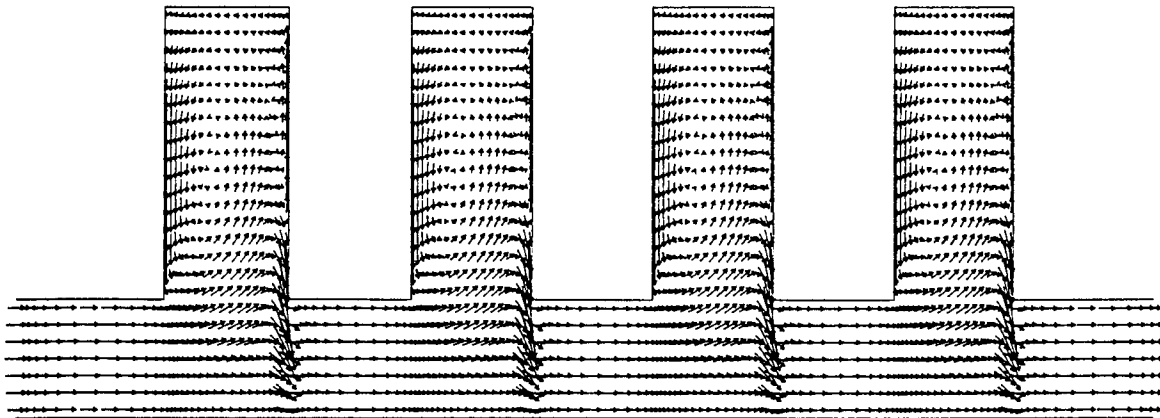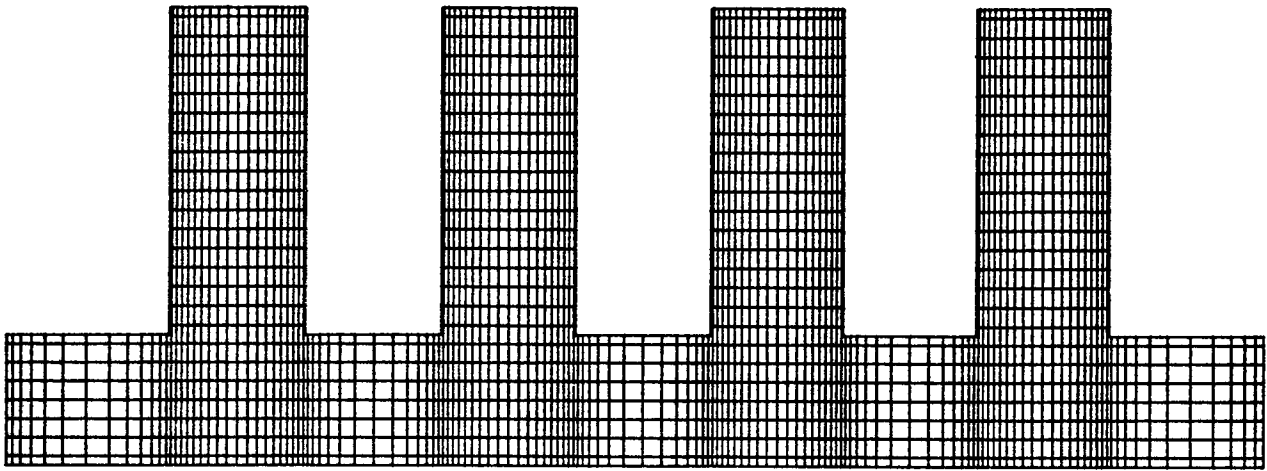Fig. 7: Comparison of the dynamic coefficients for grooved
seals.

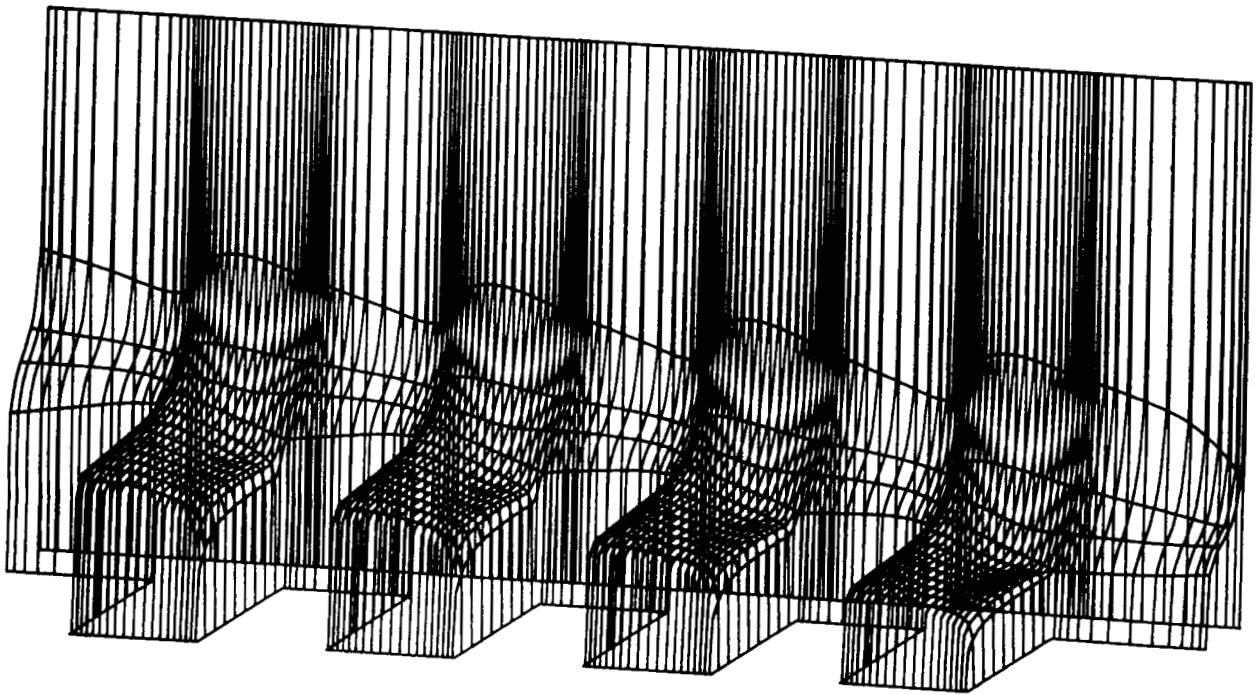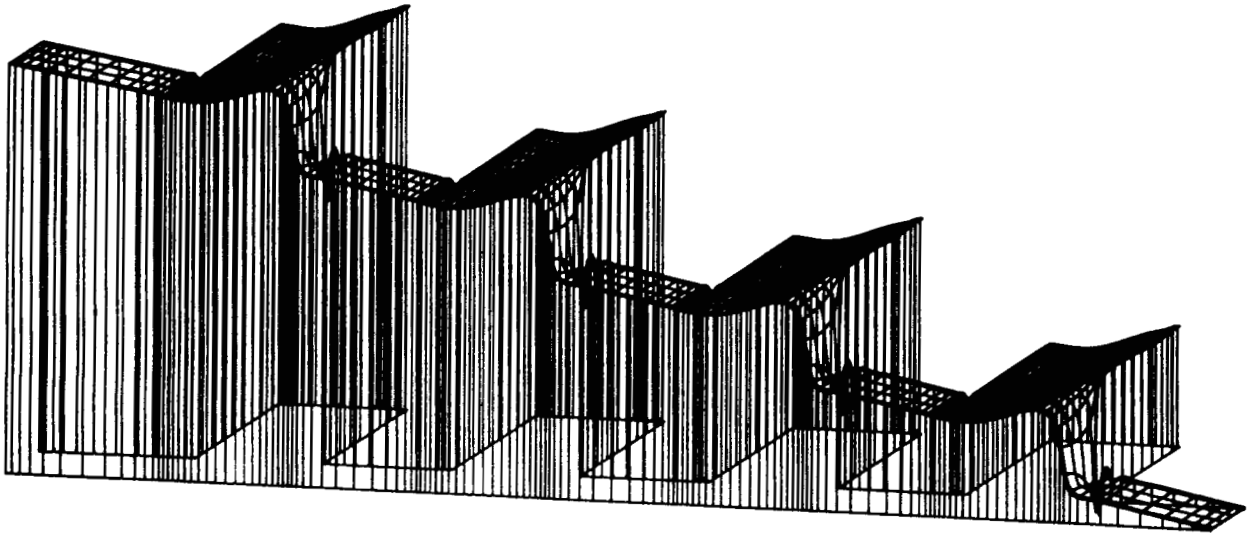Fig. 8: Grid and axial and radial velocity for a grooved
        seal

Fig. 9: Pressure distribution and circumferential velocity
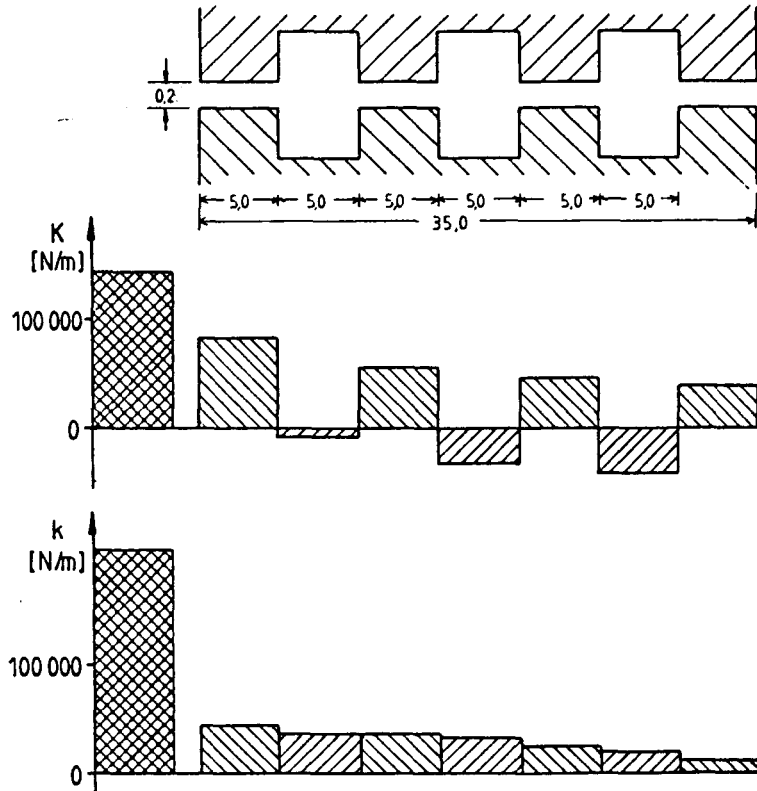for a grooved seal.

Fig. 10: Stiffness coefficients for a seal with grooves on
rotor and stator

From that diagram we can draw the following interesting conclusions:
1. Although the pressure loss for a centric shaft position has the same magnitude
    for every land part, these lands develop different contributions to the total
    coefficients.

2. Although the clearance in the chambers is 5-times greater than in the land
    parts, the forces in the chambers can't be neglected.

3. The chambers have a strong destabilizing effect, because they cause positive
    radial forces and big positive tangential forces. (positive forces have the
    direction of the z-y axes in Fig. 1)

4. Example

We made further test calculations for the seal arrangement shown in Fig. 11.
The seal data for this example are

$\mu_1 = 0.7e^{-3}$ Ns/m^2 $\xi = 0.5$

$\rho = 1000$ kg/m^3 $\overline{w}(0,\theta)/r_i\omega = 0.5$

total pressure loss   : 0.347 Mpa   n = 2000 RPM
Radius of shaft orbit : $r_o = C_o/40$

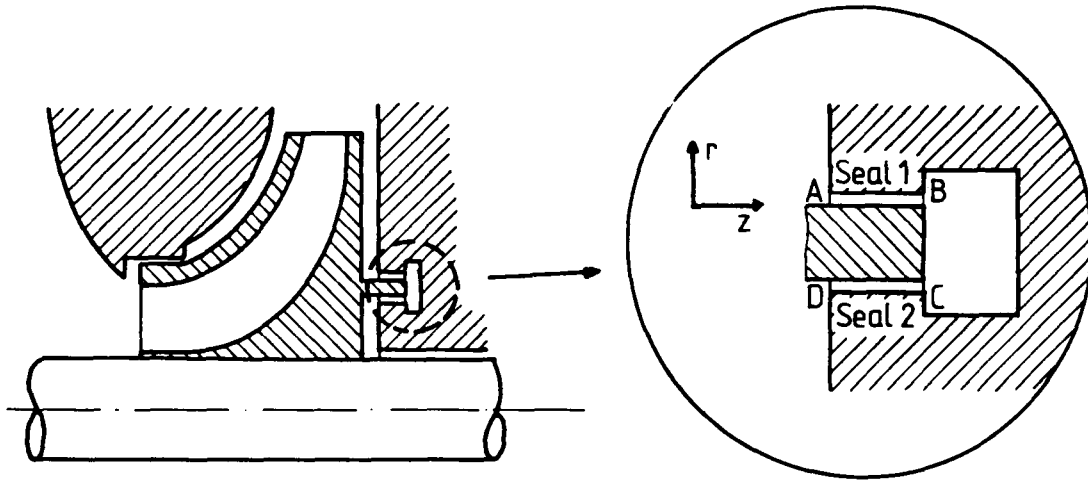223

Fig. 11: Geometry of a reversing chamber

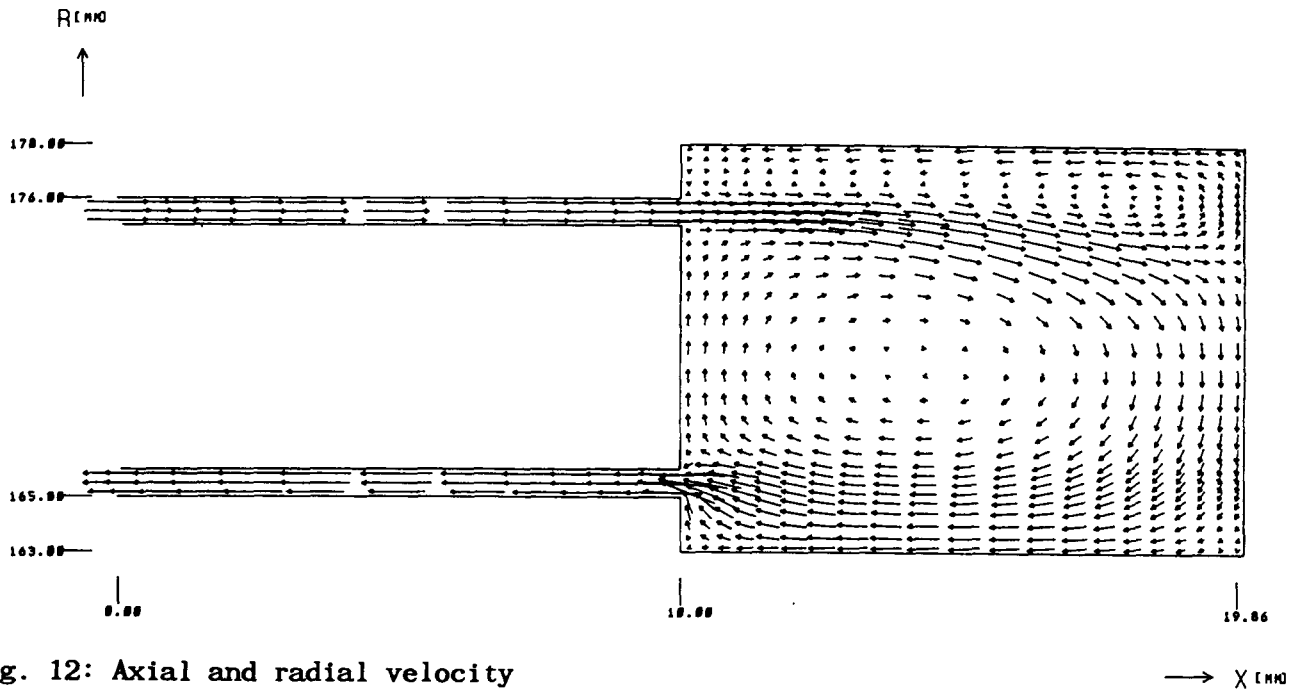In Fig. 12 the flowfield in this seal is shown.

Fig. 12: Axial and radial velocity

As a result the following stiffness coefficients for seal 1 and seal 2 (Fig. 11) are obtained.

	K [N/m]	k [N/m]
Seal 1	- 0.128 e7	- 0.133 e6
Seal 2	- 0.921 e5	- 0.853 e5

224

The result is surprising, because seal 1 yields a negative direct stiffness instead of the expected positive.
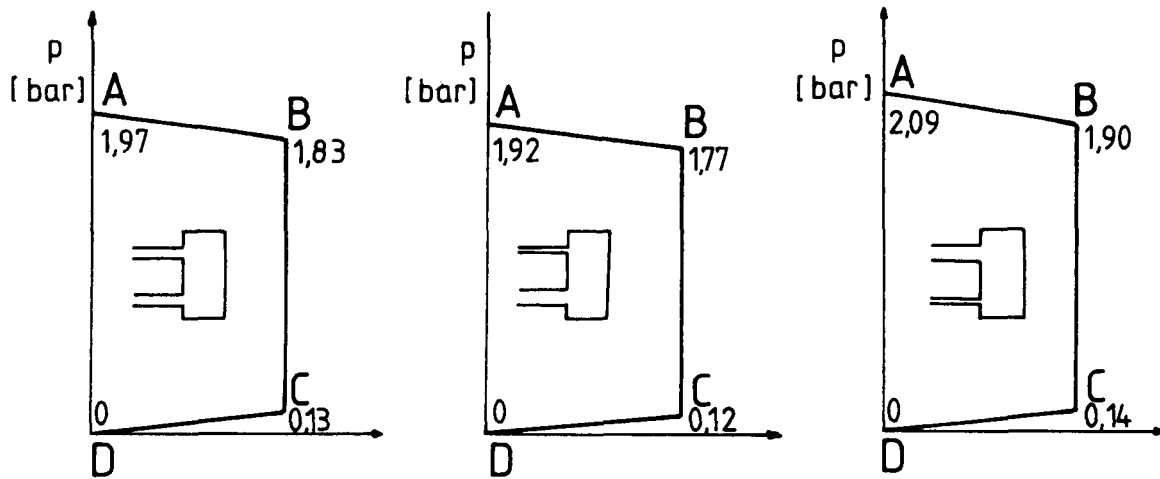This can be explained if one looks at the pressure loss in the seal arrangement.

Fig. 13: Pressure loss for   Pressure loss in the   Pressure loss in the
          centric shaft   plane with nearest   plane with widest
          position   gap in seal 1   gap in seal 1

The main pressure loss is caused by the entrance loss of the flow from the chamber into seal 2 (Fig. 13). If now, the rotating part moves in the r-direction the increase of the clearance of seal 2 (in the plane considered) results in a sharp drop in the pressure loss B–C. And this drop in the pressure loss and the rise in the opposite plane is responsible for the negative value of k in seal 1.

CONCLUSIONS

The first two examples show that the perturbation analysis yields good results in comparison with the 3-dimensional theory although it requires only a fraction of the calculation time and storage needed for that method. On the other hand it is only possible to determine the coefficients of look-through seals with the perturbation analysis, while there are no restrictions concerning the geometry for the 3-dimensional procedure.

Example 3 and 4 clearly demonstrate that in an arrangement of several seals, the separated consideration of the single seals, even with big chambers between them, may lead to totally wrong results.

F_z, F_y	Forces on the shaft in z and y direction
K, k	direct and cross-coupling stiffness
D, d	direct and cross-coupled damping
M, m	direct and cross-coupling inertia
u,v,w	axial, radial and circumferential velocity
p	pressure
k	turbulence energy
ϵ	energy dissipation
μ_e,μ_l,μ_t	effective, laminar and turbulent viscosity
ρ	density
t	time
x,r,θ	axial, radial and circumferential coordinate
G	production term in k-ϵ-model
σ_k,σ_ϵ	Constants of the k-ϵ-model
C_μ,C_1,C_2	Constants of the k-ϵ-model
ϕ	general variable standing for u,v,w,p,k ϵ
S_ϕ	general source term
C_o	seal clearance
r_o	radius of the precession motion of the shaft
$e = r_o/C_o$	perturbation parameter
ω	rotational frequency of the shaft
Ω	precession frequency of the shaft
ξ	entrance lost-coefficient
L	Length of the seal
r_i	radius of the rotor (shaft)
r_a	radius of the stator

APPENDIX A: Constants and production term of the k-ϵ model

$$C_\mu = 0{,}09 \quad C_1 = 1{,}44 \quad C_2 = 1{,}92 \quad \sigma_k = 1{,}0 \quad \sigma_\epsilon = 1{,}3$$

$$G = \mu_e \left[2\left(\left(\frac{\partial v}{\partial r}\right)^2 + \left(\frac{\partial u}{\partial x}\right)^2 + \frac{1}{r}\frac{\partial w}{\partial \theta} + \frac{v}{r}\right)^2 + \left(\frac{\partial v}{\partial x} + \frac{\partial u}{\partial r}\right)^2 + \left(\frac{1}{r}\frac{\partial v}{\partial \theta} + \frac{\partial w}{\partial r} - \frac{w}{r}\right)^2 + \left(\frac{\partial w}{\partial x} + \frac{1}{r}\frac{\partial u}{\partial \theta}\right)^2 \right]$$

REFERENCES

/1/ Childs, D.W.: Finite Length solutions for rotordynamic coefficients of turbulent annular seals. Journal of Lubrication Technology, ASME-Paper, No 82 Lub. 42, 1982

/2/ Nelson, C.C.; 1985: Rotordynamic coefficients for compressible flow in tapered annular seals. Journal of Tribology, Vol. 107, July 1985

/3/ Dietzen, F.J.; Nordmann, R.; 1987: Calculation of rotordynamic coefficients of Seals by 'Finite-Difference' techniques. ASME Journal of Tribology, July 1987

/4/ Nordmann, R.; Dietzen, F.J.; Weiser, H.P.: Calculation of Rotordynamic Coefficients and Leakage for Annular Gas Seals by Means of Finite Difference Techniques. The 1987 ASME Design Technology Conferences - 11th Biennial Conference on Mechanical Vibration and Noise. Boston, Massachusetts, September 27-30, 1987

/5/ Launder, B.E.; Spalding, D.B.: The numerical computation of turbulent flows. Computer methods in applied mechanics and engineering. 3 (1974) 269-289

/6/ Rodi, W.: Turbulence models and their application in hydraulics. Presented by the IAHR-Section on Fundamentals of Division II. Experimental and mathematical Fluid Dynamics

/7/ Stoff, H.: Calcule et mesure de La turbulence d'un ecoulement incompressible dans le Labyrinthe entre un arbre en rotation et un cylindre stationaire. Theses No. 342 (1949) Swiss Federal College of Technology, Lausanne, Juris Verlag Zürich, 1979

/8/ Wyssmann, H.R.; Pham, T.C.; Jenny, R.J.: Prediction of stiffness and damping coefficients for centrifugal compressor labyrinth seals. ASME Journal of Engineering for Gas Turbines and Power, Vol. 106, Oct. 1984

/9/ Rhode, D.L.; Demko, J.A.; Traegner, U.K.; Morrison, G.L.; Sobolik, S.R.: Prediction of incompressible flow in labyrinth seals. ASME Journal of Fluids Engineering, Vol. 108, March 1986

/10/ Wittig, S.; Jackobsen, K.; Schelling, U.; Dörr, L.; Kim, S.: Wärmeübergangszahlen in Labyrinthdichtungen. VDI-Berichte 572.1, Thermische Strömungsmaschinen '85, p. 337-356

/11/ Truckenbrodt, E., 1980: Fluidmechanik, Band 1. Grundlagen und elementare Strömungsvorgänge dichtebeständiger Fluide. Springer Verlag 1980, pp. 118-119

/12/ Gosman, A.D.; Pun, W.: Lecture notes for course entitled: 'Calculation of recirculating flows'. Imperial College London, Mech. Eng. Dept., HTS/74/2

/13/ Benodekar, R.W.; Goddard, A.J.H.; Gosman, A.D.; ISSU, R.I.: Numerical prediction of turbulent flow over surfacemounted ribs. AIAA Journal Vol. 23, No 3, March 1985

/14/ Patankar, S.V.: Numerical heat transfer and fluid flow. McGraw Hill Book Company (1980)

/15/ Maßmann, H., 1986: Ermittlung der dynamischen Parameter turbulent durchströmter Ringspalte bei inkompressiblen Medien. Vom Fachbereich Maschinenwesen der Universität Kaiserslautern zur Verleihung des akademischen Grades Doktor-Ingenieur genehmigte Dissertation

/16/ Diewald, W.; Nordmann, R., 1988: Influence of Different Types of Seals on the Stability Behavior of Turbopumps. The Second International Symposium on Transport Phenomena, Dynamics and Design of Rotating Machinery; Volume 2: Dynamics. Honolulu, Hawaii April 3-6, 1988.